

Title	Specific Behavior of Intracellular Streptococcus pyogenes That Has Undergone Autophagic Degradation Is Associated with Bacterial Streptolysin O and Host Small G Proteins Rab5 and Rab7
Author(s) Alternative	Sakurai, A; Maruyama, F; Funao, J; Nozawa, T; Aikawa, C; Okahashi, N; Shintani, S; Hamada, S; Ooshima, T; Nakagawa, I
Journal	The Journal of biological chemistry, 285(29): 22666-22675
URL	http://hdl.handle.net/10130/1939
Right	

(Revised JBC/2009/100131)

The Specific Behavior of Intracellular *Streptococcus pyogenes* Undergone the Autophagic Degradation is Associated with Bacterial Streptolysin O and Host Small G Proteins Rab5 and Rab7

Atsuo Sakurai^{1,2,3}, Fumito Maruyama⁴, Junko Funao², Takashi Nozawa^{5,6}, Chihiro Aikawa^{5,6}, Nobuo Okahashi⁷, Seikou Shintani^{1,3}, Shigeyuki Hamada⁸, Takashi Ooshima^{2*}, Ichiro Nakagawa⁶

From ¹Department of Pediatric Dentistry, Tokyo Dental College, 1-2-2 Masago, Mihama-Ku, Chiba 261-8502, Japan, ²Department of Pediatric Dentistry, Osaka University Graduate School of Dentistry, Suita, Osaka 565-0871, Japan, ³Oral Health Science Center, hrc7, Tokyo Dental College, Mihama-ku, Chiba, 261-8502, Japan, ⁴Department of Biological Information, Graduate School of Bioscience and Biotechnology, Tokyo Institute of Technology, Midori-ku, Yokohama 226-8501, Japan, ⁵Section of Bacterial Pathogenesis, Tokyo Medical and Dental University Graduate School of Medical and Dental Sciences, 1-5-45 Yushima, Bunkyo-ku, Tokyo, 113-8510, Japan, ⁶Department of Medical Genome Sciences, Graduate School of Frontier Sciences, The University of Tokyo, Kashiwa, Chiba 277-8562, Japan, ⁷Department of Oral Frontier Biology, Graduate School of Dentistry, Osaka University, 1-8 Yamadaoka, Suita-Osaka 565-0871, Japan, ⁸Research Collaboration Center on Emerging and Reemerging Infections (RCC-ERI) 6F, Department of Medical Sciences, Ministry of Public Health, Tiwanon Road, Muang Nonthaburi, 11000, Thailand.

Running head: The unique behavior of intracellular GAS.

Address correspondence to: Department of Pediatric Dentistry, Osaka University Graduate School of Dentistry, Suita, Osaka 565-0871, Japan. Fax: +81-6-6879-2965; E-mail: ooshima@dent.osaka-u.ac.jp

***Streptococcus pyogenes* (group A streptococcus: GAS) is a pathogen that invades non-phagocytic host cells, and causes a variety of acute infections such as pharyngitis. Our group previously reported that intracellular GAS is effectively degraded by the host-cell autophagic machinery, and that a cholesterol-dependent cytolysin, streptolysin O (SLO), is associated with bacterial escape from endosomes in epithelial cells. However, the details of both the intracellular behavior of GAS and the process**

leading to its autophagic degradation remain unknown. In this study, we found that two host small G proteins, Rab5 and Rab7 were associated with the pathway of autophagosome formation and the fate of intracellular GAS. Rab5 was involved in bacterial invasion and endosome fusion. Rab7 was clearly multifunctional, with roles in bacterial invasion, endosome maturation, and autophagosome formation. In addition, this study showed that the bacterial cytolysin SLO supported the escape of GAS into the

cytoplasm from endosomes, and surprisingly, a SLO-deficient mutant of GAS was viable longer than the wild-type strain although it failed to escape the endosomes. This intracellular behavior of GAS is unique and distinct from that of other types of bacterial invaders. Our results provide a new picture of GAS infection and host-cell responses in epithelial cells.

Streptococcus pyogenes (Group A streptococcus; GAS) is the causative pathogen for a diverse collection of human diseases, such as pharyngitis, bacteremia, and necrotizing them. This system is important for the physiological turnover of cytoplasmic components, and is involved in a number of clinical conditions and diseases (6,7). Recently, we and others showed that GAS is captured and degraded by autophagy, not by the endosome-lysosome system (8,9). Some species of bacteria invade host non-phagocytic cells, such as epithelial cells, and are largely degraded by the endocytosis pathway (10-12). However, some bacteria, including *Listeria monocytogenes*, *Shigella flexneri*, *Mycobacterium tuberculosis*, and *Salmonella typhimurium*, cannot be eliminated by endosomes, and replicate within the cytoplasm (13-15). The autophagic machinery is thought to act to remove these bacteria. However, it is still unclear under what circumstances the intracellular bacteria are sequestered by autophagosomes and what events in the infected cells lead to the degradation of bacteria by autophagy.

A cholesterol-dependent cytolysin of GAS, SLO, is a homolog of listeriolysin O (LLO) in *L. monocytogenes*. LLO is involved in the bacterial escape from phagosomes in

fasciitis (1). GAS strains produce a variety of pathogenic factors such as streptolysin O (SLO), superantigens, and DNase (2-4). Invasive GAS diseases occur in approximately 1/1000 cases, with associated mortality of 25% (5).

Autophagy is defined as 'self-eating', bulk degradation system for cytoplasmic components. During autophagy, double membrane structures are formed in the cytoplasm, in which cytoplasmic organelles and proteins are sequestered. These structures, called autophagosomes, subsequently fuse with lysosomes to degrade the components within macrophages (16,17). It is known that SLO and LLO share 60% amino acid identity, and that their three-dimensional structures and characteristic domains are highly conserved. Although SLO was reported to be a critical factor for bacterial escape from endosomes, it has not been known whether and how SLO is involved in the subversion process of endosomes (8,18). Thus, we examined whether SLO promotes the bacterial escape from endosomes, as well as how SLO induces autophagy in GAS-infected host cells.

When extracellular materials enter a host cell through the endocytic pathway, Rab proteins, which regulate membrane trafficking in mammalian cells, are recruited (19,20). Rab proteins belong to the small G protein superfamily and have GTP/GDP-binding and GTPase activities. GTP-bound active Rab proteins interact with specific effectors and participate in the formation and motility of transport vesicles, as well as their fusion with endosomes (21). Among the Rab proteins, Rab5 and Rab7 which are involved in the endosomal pathway, play crucial roles in the fusion of

endosomes and in their maturation to lysosomes, respectively (22-24). In addition, Rab7 was reported to be associated with the maturation of autophagosomes under amino acid starvation conditions (25). Therefore, the influences of Rab5 and Rab7 should be also analysed in detail during GAS infection.

In this study, we examined the behavior of GAS within host epithelial cells prior to bacterial elimination by the autophagic pathway. Additionally, the influences of the bacterial SLO and host Rab proteins on the fate of intracellular GAS were also studied.

Experimental procedures

Construction of a slo-deficient mutant and complemented strains of GAS— GAS JRS4 (serotype M6) and its mutant strains were used for this study (Supplemental table S1) (12,26). A *slo*-deficient mutant strain, JRS4 Δ *slo* was constructed by electroporation, as described previously (3). Briefly, JRS4 was transformed with a suicide vector pSF151-fSLO, which was pSF151 containing an internal fragment of the *slo* gene (27,28). For a complemented strain of JRS4 Δ *slo*, JRS4 Δ *slo*-comp, the intact *slo* gene-ligated pENTR-SD-TOPO (Life Technologies) and pOGW vector, containing an isopropyl β -D-1-thiogalactopyranoside (IPTG)-inducible promoter and adapted for the Gateway system, were subjected to a recombination reaction using LR clonase (Life Technologies) (29). The resulting pOGW-SLO was introduced into JRS4 Δ *slo* by electroporation. Transformants were verified by PCR (Supplementary table S2) and by the determination of SLO-specific hemolytic titers

(28). The expression of the SLO protein in JRS4 Δ *slo*-comp was induced by 1 mM IPTG for 2 h and verified by Coomassie blue staining and immunoblots using a specific anti-peptide antibody, raised using White New Zealand rabbits against a 14-amino acid peptide (ENKPDVVTKRNPQ), corresponding to residues 190-203 of the SLO amino acid sequence.

Construction of plasmids for visualizing host cellular proteins— Plasmids expressing proteins fused with a fluorescent protein were constructed to detect the induction of endosomes and autophagosomes (Supplemental table S1). Rat microtubule-associated protein 1 light chain 3 (LC3; a marker of autophagosomes), Rab5, and Rab7 (markers of endosomes) were fused with enhanced green fluorescence protein (EGFP) or a red fluorescent protein (mCherry) (30,31). The dominant-active (DA) form of Rab5 (Rab5Q79L), dominant-negative (DN) form of Rab5 (Rab5S34N), DA form of Rab7 (Rab7Q67L), and DN form of Rab7 (Rab7T22N) were then constructed using the PrimeSTAR Mutagenesis Kit (Takara Shuzo) (Supplemental Tables S1 and S2) (32-34). For the transfection of cultured cells without adenovirus, these expression plasmids were introduced with the Fu gene HD reagent (Roche) for 6 h. The cells were further incubated for 48 h and then used for experimental assays.

For the transfection of cells with these genes using adenovirus vector, Gateway vectors such as pENTR11 and pAd/CMV/V5-dest were used (Life Technologies) (Supplemental table S1). Then, the linearized plasmids were transfected into human embryonic kidney-derived 293A cells according to the supplier's instructions (35). The titers of viruses

were enhanced by repeated passaging until more than 90% of the cells produced fluorescence.

Bacterial infection assay— For GAS infection, bacteria grown to the mid-log phase were harvested and washed twice with phosphate buffered saline (PBS; pH 7.4). Human cervical epithelial HeLa cells (ATCC CCL-2) incubated in a 24-well plate using 10% fetal calf serum-containing DMEM were infected with GAS strains at 2×10^6 colony-forming units (CFUs) per well (multiplicity of infection = 100), except for the bacterial invasion and viability assays, in which the cells were seeded at a density of 1×10^5 cells per well and were infected with 1×10^7 CFU. After 1 h, the cells were washed with PBS and were further cultured with 100 $\mu\text{g}/\text{ml}$ gentamicin and 100 U/ml penicillin G to remove extracellular bacteria. The times shown in the text and in all figures indicate the elapsed time after the infection procedure was started. Where indicated, cells were pre-infected with recombinant adenoviruses or transfected with protein-expressing plasmids for 48 h prior to their infection with GAS.

Microscopic observations— For confocal microscopy, cells infected with GAS strains were fixed with 4% paraformaldehyde in PBS for 3 h at 4 °C. Mouse monoclonal anti-human lysosome associated membrane protein-1 (LAMP-1; a lysosomal marker) (clone H4A3; Santa Cruz Biotechnology), anti-early endosomal antigen (EEA)-1 (Becton Dickinson), anti-cathepsin D (Sigma), or anti-SLO antibodies were used as the primary antibodies for immunostaining. The secondary antibody was Cy5-conjugated anti-mouse IgG or anti-rabbit IgG (Jackson ImmunoResearch). To label bacterial and cellular DNA, 0.2 $\mu\text{g}/\text{ml}$ propidium iodide (PI; Sigma) or

2 $\mu\text{g}/\text{ml}$ 4', 6-diamino-2-phenylindole (DAPI; Sigma) in PBS was used. All fluorescence micrographs were confocal images acquired with a Fluoview FV1000 confocal microscope (Olympus).

For electron microscopy, cells infected with GAS were fixed with 2.5% glutaraldehyde in 0.1 M cacodylate (pH 7.4) for 2 h. Conventional electron microscopy was performed as previously described (7). Briefly, cells were pelleted, embedded in 7.5% gelatin in PBS, and infused with 2 M sucrose for 30 min. Ultrathin sections were stained by uranyl acetate plus lead citrate and were observed with an H7600 electron microscope (Hitachi).

Measurement of GAS-containing autophagosomes and endosomes— To estimate the induction of autophagy in GAS-infected cells, the percentage of GAS-invaded cells that contained LC3-positive autophagosomes was determined. At least 500 cells were observed to examine the formation of autophagosomes under the confocal microscope. The percentage of LC3-positive cells compared to cells invaded by GAS was determined in each experiment. In the case of endosomes, the ratio of GAS trapped within Rab5-positive compartments to total intracellular GAS was determined by area calculations of GAS using Image-J 1.41 software (Wayne Rasband; the Research Services Branch, National Institute of Mental Health), based on confocal images (8). At least 20 cells were analyzed at each time point.

Bacterial invasion and viability assays— Cells in a 24-well plate were infected with GAS for 1 h and then incubated with antibiotics for an additional 10 minutes for bacterial invasion assays (total incubation was 1 h and 10 min after

infection) or for 2 or 4 h (for bacterial viability assays; total incubation of 3 or 5 h after infection). Next, the cells were washed with PBS and disrupted in sterile distilled water, and serial dilutions of the lysates were spread on THY agar plates as described previously (36). For bacterial invasion assays, the amount of intracellular GAS at the point of cell disruption was expressed as the percentage of total bacteria added to the cell culture. For bacterial viability assays, the data are shown as the percentage of live GAS after 3 or 5 h in comparison with the viable cells detected at 1 h and 10 min after infection.

Statistics— All data are presented as the means of triplicate assays of a representative experiment \pm standard error. Statistical analyses were carried out by Students' *t*-test, Scheffe's test, and chi-square test using JMP software (SAS Institute, Cary, NC). $P < 0.05$ was considered to be significant.

RESULTS

Localization of early and late endosomal membrane markers over time in GAS-infected cells. HeLa cells expressing fluorescently labeled Rab5 were infected with GAS strain JRS4, and endocytosis was monitored during the JRS4 invasion. Confocal microscopy showed that JRS4 invaded the cells and was trapped by Rab5-positive early endosomes 1 h after infection. However, JRS4 started to escape from the early endosomes 2 h after infection, and the number of bacteria in the cytoplasm increased in a time-dependent manner (Fig. 1A, left panels and Supplemental fig. S1). The number of JRS4 cells remaining within the early endosomes did not change for up to 3 h after infection, but decreased

slightly by 4 h (Fig. 1B, open circles). Although many bacteria were present in the cytoplasm at 3 h by confocal imaging, the decrease in JRS4 in the endosomes was not apparent at that time point (Fig. 1B). It should be noted that some bacteria invaded the host cells incompletely at 1 h and were not entirely trapped by the Rab5-positive vacuoles.

Although Rab7 has been used as a marker of late endosomes, Rab7-positive compartments containing JRS4 could also be seen in host cells throughout the observation period, including at early time points (Fig. 1A, right panels and Supplemental fig. S1). Intracellular JRS4 that was not sequestered by Rab7-positive compartments was also observed at 2, 3, and 4 h after infection. Because Rab7-positive compartments were found at early stages of infection, the data suggest that Rab7 presents in the cytoplasm in the absence of visible endosomes or has functions other than as a membrane protein in late endosomes in GAS-infected cells.

Autophagosomes are formed in the vicinity of early endosomes. Since intracellular JRS4 is sequestered and degraded by the autophagic machinery (8), we next determined when the autophagic machinery was induced in cells infected with JRS4, and how autophagosomes were formed in these cells. In cells co-expressing Rab5 and LC3, LC3-positive autophagosomes became gradually visible by 2 h after infection and were more evident at later stages (Fig. 2A and Supplemental fig. S2A). JRS4 that was sequestered by autophagosomes was also trapped within Rab7-positive compartments, but not within early endosomes. (Figs. 2A and B, and Supplemental figs. S2A and B). In addition, JRS4

associated with Rab7-positive compartments was not sequestered by autophagosomes, and some bacteria were found in the cytoplasm 3 or 4 h after infection (Fig. 2B). These observations suggested two possibilities regarding the autophagosome formation: i) the autophagic machinery was induced to destroy the bacteria that had escaped from endosomes into the cytoplasm, or ii) autophagosomes trapped the bacteria contained within endosomes that had undergone the replacement of Rab5 with Rab7.

In order to see how autophagosomes sequestered bacteria, we performed electron microscopy. It showed that when JRS4 invaded the host cells, the bacteria were trapped in the characteristic single-membrane structures of endosomes (Fig. 2C). However, the JRS4 gradually escaped from the endosomes and were present in the cytoplasm, where multi-membrane-bound structures containing bacteria were observed 3 h after infection (Fig. 2C). These structures were autophagosomes that contained inclusions of the cytoplasmic-side multi-membrane. These data indicated that autophagosomes sequestered the cytosolic GAS that escaped from endosomes, and did not surround the GAS-containing intact endosomes.

Rab5 and Rab7 involvement in autophagosome formation. To analyze the functions of Rab5 and Rab7 in GAS-infected cells, dominant active and dominant negative forms of Rab proteins were constructed, i.e., plasmids expressing Rab5Q79L (DA form of Rab5), Rab5S34N (DN form of Rab5), Rab7Q67L (DA form of Rab7), and Rab7T22N (DN form of Rab7). The number and size of the early endosomes in cells expressing Rab5Q79L were significantly greater than those of cells expressing wild-type Rab5 (Fig. 3A, left

panels and Supplemental fig. S3). Cells expressing Rab5Q79L, like those expressing wild-type Rab5, contained JRS4 that had escaped from endosomes, but more bacteria remained trapped in the endosomes than in Rab5-expressing cells (Figs. 1A and 3A). There was no significant difference between the number of bacteria in cells expressing wild-type Rab5 and Rab5Q79L, but the cells expressing Rab5Q79L tended to contain more invading bacteria (Fig. 3B). Endosomal structures containing JRS4 were evident even 4 h after infection in the cells expressing Rab5Q79L (Fig. 3A). In cells expressing Rab5S34N, the bacterial invasion was remarkably reduced compared to cells expressing wild-type Rab5 (Fig. 3B). Moreover, the Rab5S34N expression was rather diffuse, and no endosomal structures containing JRS4 were seen in these cells at any point in the observation period (Supplemental fig. S4A). These findings suggested that Rab5 is involved not only in bacterial invasion, but also in the formation and fusion of endosomes in JRS4-infected cells.

In cells expressing Rab7Q67L, Rab7-positive compartments that trapped intracellular JRS4 appeared 1 h after infection (Fig. 3A, right panels and Supplemental fig. 3A), as in the cells expressing wild-type Rab7 (Fig. 1A, right panels). Moreover, most of the Rab7-positive compartments that contained bacteria fused with lysosomes, as indicated by LAMP-1 staining, at the early stage of infection. Compared to cells expressing wild-type Rab7, intracellular bacteria were slightly, but not significantly, elevated in cells expressing Rab7Q67L (Fig. 3B). By contrast, in cells expressing Rab7T22N, the Rab7-positive compartments did not form, and the aggregation

of lysosomes did not occur (Supplemental fig. S4B). The amount of intracellular bacteria in cells expressing Rab7T22N was significantly less than in cells expressing wild-type Rab7 (Fig. 3B and Supplemental fig. S4B). Thus, not only Rab5 but also Rab7 appeared to be associated with bacterial invasion. In addition, Rab7 might be involved in the fusion of endosomal structures with lysosomes.

The fate of the GAS within the host cells depended on whether or not bacteria escaped from the endosomes. We studied their fate by using a specific antibody against LAMP-1. At 3 and 4 h after infection, LAMP-1 was co-localized with autophagosomes, but not with Rab5-positive endosomes (Figs. 4A and B, and Supplemental fig. S5A and S5B). We found that lysosomes accumulated in a time-dependent manner and fused with the autophagosomes rather than with the Rab5-positive endosomes. Furthermore, immunostaining for cathepsin D, a proteolytic enzyme of lysosomes, showed that cathepsin D was present in autophagosomes (Supplemental fig. S5C). These observations indicated that, although JRS4 can escape from early endosomes, its escape rapidly induces the autophagosome-lysosomal pathway.

Intracellular GAS escapes from endosomes mediated by SLO, but the autophagic machinery degrades GAS effectively. The involvement of the secretory cytolysin SLO in the induction of autophagy was examined using JRS4 Δ slo and JRS4 Δ slo-comp. The expression of a recombinant SLO protein (MW: 69 KDa) in *E. coli* DH10B and GAS strains was detected by PCR and Western blot analyses (Supplemental figs. S6A and B). We detected autophagosomes by expressing fluorescently labeled LC3 in the

cells. When these cells were infected with JRS4 Δ slo, autophagosomes rarely formed, even 4 h after infection, despite a similar level of invasion as with wild-type JRS4 (Fig. 5A and Supplemental fig. S7A). Lysosomes containing intracellular JRS4 Δ slo were observed in some of the infected cells, but they did not co-localize with autophagosomes (Fig. 5A). Some lysosomes appeared to fuse with endosomes, but not autophagosomes, in cells infected with JRS4 Δ slo. Moreover, JRS4 Δ slo-comp induced autophagy in cells expressing LC3, just as wild-type JRS4 did (Fig. 5B, shown in green and red, and Supplemental fig. S7B). Whereas autophagy had been induced in 80% of cells infected with wild-type JRS4 by 3 h after infection, only 10% of the JRS4 Δ slo-infected cells formed autophagosomes (Fig. 5C), but cells infected with JRS4 Δ slo-comp showed considerable recovery of their ability to induce autophagy compared with those infected with JRS4 Δ slo (Fig. 5C). Thus, our results support the idea that GAS can escape from endosomes by expressing SLO, but the cytoplasmic GAS was then sequestered by the autophagosome-lysosomal system.

To assess whether intracellular GAS trapped within endosomes was degraded by the endosome-lysosomal system at early stages of infection, the number of viable intracellular bacteria was determined. Wild-type JRS4 was degraded more rapidly than JRS4 Δ slo at 3 h after infection (Fig. 6A). More than 60% of the JRS4 Δ slo was degraded at 5 h after infection, which was later than when JRS4 reached the same degree of degradation (Fig. 6A). In host cells expressing Rab5 or Rab7, JRS4 was degraded more rapidly than JRS4 Δ slo, and the degradation rates were not significantly altered

by the expression of intact Rab5 or Rab7 (Figs. 6B-E). However, cells expressing Rab5Q79L did not degrade JRS4 Δ slo effectively, even at 5 h (Fig. 6C). This might have been because gradual inactivation and replacement of Rab7 did not occur in these cells. On the other hand, both JRS4 and JRS4 Δ slo were eliminated effectively in cells expressing Rab7Q67L (Fig. 6D). These findings indicate that both Rab5 and Rab7 modulate the progression of endosome maturation in GAS-infected cells.

We next examined the effects of SLO expression on early endosomes. In cells expressing Rab5, JRS4 Δ slo was contained in early endosomes like the wild-type JRS4, but the bacteria did not escape the endosomes even 3 or 4 h after infection (Fig. 7A and Supplemental fig. S8A). Similar results were observed in the Rab5Q79L-expressing cells (Supplemental fig. S9A). The proportion of GAS within the early endosomes among the total number of intracellular bacteria was significantly different between JRS4 and JRS4 Δ slo (Fig. 1B). In cells expressing Rab7, JRS4 Δ slo was trapped by Rab7-positive compartments throughout the observation period (Supplemental fig. S9B). Electron microscopy showed that the intracellular JRS4 Δ slo was enclosed by single membrane structures (indicating endosomes), and free bacteria were not found in the cytoplasm (Supplemental fig. S9C). Furthermore, no autophagosomes that sequestered JRS4 Δ slo was observed.

The positional relationship between the early endosomes and autophagosomes in the cells was investigated using an antibody against EEA-1. At 2 h after infection, JRS4 and JRS4 Δ slo-comp were found in autophagosomes

adjacent to early endosomes, whereas almost all JRS4 Δ slo still resided in endosomes and not in autophagosomes (Fig. 5B). Subsequently, SLO was detected within endosomes in JRS4-infected cells at 2 h after infection, but not in JRS4 Δ slo-infected cells (Fig. 7B and Supplemental fig. S8B). These results indicated that the expression and accumulation of SLO acts directly on the pore formation of early endosomes in JRS4-infected cells and facilitates bacterial escape, leading to bacterial entry into the cytoplasm.

DISCUSSION

From these results, we obtained a comprehensive view of the pathway leading to autophagosome formation after GAS invasion, which involves endosome formation, GAS escape into the cytoplasm, and GAS degradation by the autophagosome-lysosomal pathway. This overall pathway is summarized in Fig. 8. The involvement of both GDP- and GTP-bound form of Rab5 and Rab7 in this pathway is also described. SLO promotes the escape of GAS from endosomes, however bacteria are sequestered.

GAS is reported to be capable of invading host cells via endocytosis, a process involving several bacterial fibronectin-binding proteins (e. g.; F protein and FbaB) (11,12,37). The main purpose of this study was to elucidate the fate of GAS after its invasion into host cells. To achieve this, Rab5 and Rab7 were used as markers of early and late endosomes, respectively (23,38-41). Rab5 was reported to localize to the membranes of early endosomes, activating Rab7 and promoting the Rab5-Rab7 exchange (24,42).

Rab7 is presumed to promote the fusion of endosomes with lysosomes (23).

First, the movement of the invading JRS4 in cells expressing Rab5 or Rab7 was analyzed using confocal microscopy. Although Rab7 is known to be a specific marker of late endosomes, our study showed that Rab7-positive compartments were seen throughout the observation period (Fig. 1A). If Rab7 associated only with the membranes of late endosomes, the results suggest that the emergence of Rab7-positive compartments occurred in conjunction with early endosomes. Alternatively, Rab7 might function in roles besides the promotion of endosome-lysosome fusion, such as the uptake of GAS (40). Under the electron microscope, intracellular JRS4 was seen in endosomes, however, the bacteria gradually escaped into the cytoplasm. Next, autophagosomes, which are characterized as containing cytoplasm inside multimembrane structures, began to emerge and sequester JRS4 (Fig. 2C) (30,43). These observations confirmed that autophagosomes formed within cells in response to the bacterial infection.

It was reported that intracellularly invading *M. tuberculosis* is sequestered by autophagosomes, which surround not only the bacteria but also endosomal membranes (44). *L. monocytogenes* possessed a cytolysin LLO, a homolog of SLO of GAS. This bacterium was reported to escape from phagosomes into the cytoplasm using LLO and to evade autophagy by using another bacterial protein named ActA (45,46). The intracellular behavior of *L. monocytogenes* is different from that of GAS, because the ActA facilitates its motility and cell-to-cell spread by polymerizing the host cell

actin (47). Furthermore, *L. monocytogenes* can form *Listeria*-containing phagosomes (SLAPs) in host macrophages and replicate within these vacuoles under conditions of low LLO expression (48). An intracellular obligate parasite, *Coxiella burnetii*, has an ability to replicate within intracellular vacuoles that are altered phagosomes and recruits Rab5 and Rab7 quickly to facilitate its uptake and vacuole development (49). Therefore, the behavior of GAS in host cells found in the present study was different from the strategies reported previously for other bacteria.

We also studied the functions of Rab proteins in GAS-infected cells using DN mutant form Rab5 and Rab7 (33,34). The number of early endosomes in cells expressing DA form of Rab5 (Rab5Q79L) was significantly greater than in cells expressing wild-type Rab5 (Fig. 3A, left panels). This finding was consistent with a previous report that examined the uptake of transferrin in cells expressing Rab5Q79L (22). The inhibition of Rab5 GTPase activity may prevent the dissociation of Rab5 and its downstream events, including the Rab5-Rab7 exchange (22). In contrast, Rab5Q79L was reported to induce the rapid recruitment of Rab7, but failed to displace Rab5 during low-density lipoprotein uptake (24). Others have reported that Rab5Q79L restricted the viability of *L. monocytogenes* within phagosomes (50). In this study, although the elimination of JRS4 Δ slo occurred more slowly than that of JRS4, Rab5Q79L delayed its elimination even further (Fig. 6C). If Rab5Q79L promotes the Rab7 recruitment and lysosome fusion with endosomes, the intracellular GAS should have degraded rapidly, but this is not what we observed.

In the case of Rab7, our result using

DA form of Rab7 (Rab7Q67L) was consistent with a previous study showing that Rab7Q67L up-regulated the fusion of endosomes with lysosomes (Fig. 6D) (23). It is likely that GAS was degraded not only by the autophagic machinery, but also by the endosome-lysosomal pathway in the cells expressing Rab7Q67L. Furthermore, DN mutants of Rab5 and Rab7 were reported to reduce the invasion of *Trypanosoma cruzi* in CHO cells (20). This study also showed that both Rab5S34N and Rab7T22N decreased the invasion of GAS (Fig. 3B). On the other hand, the overexpression of Rab7T22N is reported to show does not influence the internalization of horseradish peroxidase or paramyxovirus SV5 protein (34).

Whereas our findings indicated that Rab5 was involved in both the fusion of endosomes and the uptake of GAS when cells were infected, involvement of Rab7 in the induction of endosomes may depend on the proteins or specific cellular receptors involved in the bacterial infection. Rab7 is also thought to be involved in the maturation of autophagosomes (25,51). The present data suggested that Rab7 is localized to both endosomes and autophagosomes and is involved in the fusion of membrane structures with lysosomes (Figs. 2B and 6D). Thus, Rab7 showed multiple functions when the cells were infected with GAS strains. Furthermore, until GAS was eliminated by the autophagic machinery, the behavior of the intracellular bacteria was strongly influenced by Rab5 and Rab7 expression.

Bacterial cytolysin SLO is known to trigger multiple cellular responses, such as the induction of inflammatory cytokines and apoptosis (52-54). Although SLO is clearly a

pathogenic factor of GAS, it seems counterintuitive that GAS expressing SLO are degraded more quickly than SLO-deficient mutants (Fig. 6A). However, we found that JRS4 Δ slo remained within endosomes for long periods and could not be eliminated efficiently by the endosome-lysosomal pathway (Fig. 6A). It seems that the autophagic machinery is more effective than endosome-lysosomal pathway against intracellular GAS. Although it is not clear whether GAS can elude autophagy like *S. flexneri* (55), the behavior of GAS within host cells appears to be unique. In contrast to GAS, it was also reported that autophagy did not affected the fate of intracellular *L. monocytogenes* in macrophages (49,56). The ability of GAS that provokes the autophagosome formation leads to degrade itself after all. This phenomenon indicates that GAS has only an insufficient system for the evasion of intracellular host defense. However, a bacterial viability assay showed that small numbers of GAS were recovered from cells even 24 and 48 h after infection even under the effective bacterial killing (data not shown). In this regard, it is reported that the in vivo entry of GAS into host cells contributes to a bacterial persistence despite antibiotic therapy for a long term (12,57). There might be another unique strategy of GAS to survive in host cells. In any case, our data support the idea that the autophagosome formation is effective for eliminating intracellular GAS and is influenced by SLO-dependent bacterial escape from endosomes.

GAS-induced autophagy is likely to be a mechanism derived specifically and selectively against intracellular bacteria, although autophagy has been identified as a non-specific

and bulk degradation pathway for cytoplasmic components (58,59). If autophagy is controlled by specific molecules, such as hormones or cytokines, medical treatments against infectious diseases could be designed to take advantage of this regulation. Therefore, further studies on the mechanisms leading to autophagosome formation in bacteria-infected epithelial cells and the corresponding host responses should be pursued.

References

1. Bisno, A. L., Brito, M. O., and Collins, C. M. (2003) *Lancet Infect Dis* **3**, 191-200
2. Lukomski, S., Sreevatsan, S., Amberg, C., Reichardt, W., Woischnik, M., Podbielski, A., and Musser, J. M. (1997) *J Clin Invest* **99**, 2574-2580
3. Madden, J. C., Ruiz, N., and Caparon, M. (2001) *Cell* **104**, 143-152
4. Buchanan, J. T., Simpson, A. J., Aziz, R. K., Liu, G. Y., Kristian, S. A., Kotb, M., Feramisco, J., and Nizet, V. (2006) *Curr Biol* **16**, 396-400
5. Carapetis, J. R., Steer, A. C., Mulholland, E. K., and Weber, M. (2005) *Lancet Infect Dis* **5**, 685-694
6. Kuma, A., Hatano, M., Matsui, M., Yamamoto, A., Nakaya, H., Yoshimori, T., Ohsumi, Y., Tokuhisa, T., and Mizushima, N. (2004) *Nature* **432**, 1032-1036
7. Yoshimori, T., Yamagata, F., Yamamoto, A., Mizushima, N., Kabeya, Y., Nara, A., Miwako, I., Ohashi, M., Ohsumi, M., and Ohsumi, Y. (2000) *Mol Biol Cell* **11**, 747-763
8. Nakagawa, I., Amano, A., Mizushima, N., Yamamoto, A., Yamaguchi, H., Kamimoto, T., Nara, A., Funao, J., Nakata, M., Tsuda, K., Hamada, S., and Yoshimori, T. (2004) *Science* **306**, 1037-1040
9. Ogawa, M., and Sasakawa, C. (2006) *Cell Microbiol* **8**, 177-184
10. Kornfeld, S., and Mellman, I. (1989) *Annu Rev Cell Biol* **5**, 483-525
11. Terao, Y., Kawabata, S., Kunitomo, E., Murakami, J., Nakagawa, I., and Hamada, S. (2001) *Mol Microbiol* **42**, 75-86
12. Sakurai, A., Okahashi, N., Nakagawa, I., Kawabata, S., Amano, A., Ooshima, T., and Hamada, S. (2003) *Infect Immun* **71**, 6019-6026
13. Falkow, S. (1991) *Cell* **65**, 1099-1102
14. Gruenheid, S., and Finlay, B. B. (2003) *Nature* **422**, 775-781
15. Nguyen, L., and Pieters, J. (2005) *Trends Cell Biol* **15**, 269-276
16. Beauregard, K. E., Lee, K. D., Collier, R. J., and Swanson, J. A. (1997) *J Exp Med* **186**, 1159-1163
17. Hara, H., Tsuchiya, K., Nomura, T., Kawamura, I., Shoma, S., and Mitsuyama, M. (2008) *J Immunol* **180**, 7859-7868
18. Amano, A., Nakagawa, I., and Yoshimori, T. (2006) *J Biochem* **140**, 161-166
19. Novick, P., and Zerial, M. (1997) *Curr Opin Cell Biol* **9**, 496-504
20. Wilkowsky, S. E., Barbieri, M. A., Stahl, P. D., and Isola, E. L. (2002) *Biochem Biophys Res Commun* **291**, 516-521
21. Pfeffer, S. (2003) *Cell* **112**, 507-517
22. Stenmark, H., Parton, R. G., Steele-Mortimer, O., Lutcke, A., Gruenberg, J., and Zerial, M. (1994) *Embo J* **13**, 1287-1296
23. Bucci, C., Thomsen, P., Nicoziani, P., McCarthy, J., and van Deurs, B. (2000) *Mol Biol Cell* **11**, 467-480
24. Rink, J., Ghigo, E., Kalaidzidis, Y., and Zerial, M. (2005) *Cell* **122**, 735-749
25. Jäger, S., Bucci, C., Tanida, I., Ueno, T., Kominami, E., Saftig, P., and Eskelinen, E. L. (2004) *J*

- Cell Sci* **117**, 4837-4848
26. Jadoun, J., Ozeri, V., Burstein, E., Skutelsky, E., Hanski, E., and Sela, S. (1998) *J Infect Dis* **178**, 147-158
 27. Tao, L., LeBlanc, D. J., and Ferretti, J. J. (1992) *Gene* **120**, 105-110
 28. Ruiz, N., Wang, B., Pentland, A., and Caparon, M. (1998) *Mol Microbiol* **27**, 337-346
 29. Ishikawa, S., Kawai, Y., Hiramatsu, K., Kuwano, M., and Ogasawara, N. (2006) *Mol Microbiol* **60**, 1364-1380
 30. Kabeya, Y., Mizushima, N., Ueno, T., Yamamoto, A., Kirisako, T., Noda, T., Kominami, E., Ohsumi, Y., and Yoshimori, T. (2000) *Embo J* **19**, 5720-5728
 31. Shaner, N. C., Campbell, R. E., Steinbach, P. A., Giepmans, B. N., Palmer, A. E., and Tsien, R. Y. (2004) *Nat Biotechnol* **22**, 1567-1572
 32. Ridley, A. J., and Hall, A. (1992) *Cell* **70**, 389-399
 33. Li, G., and Stahl, P. D. (1993) *J Biol Chem* **268**, 24475-24480
 34. Feng, Y., Press, B., and Wandinger-Ness, A. (1995) *J Cell Biol* **131**, 1435-1452
 35. Miyake, S., Makimura, M., Kanegae, Y., Harada, S., Sato, Y., Takamori, K., Tokuda, C., and Saito, I. (1996) *Proc Natl Acad Sci U S A* **93**, 1320-1324
 36. Sakurai, A., Okahashi, N., Maruyama, F., Ooshima, T., Hamada, S., and Nakagawa, I. (2008) *Biochem Biophys Res Commun* **373**, 450-454
 37. Terao, Y., Kawabata, S., Nakata, M., Nakagawa, I., and Hamada, S. (2002) *J Biol Chem* **277**, 47428-47435
 38. Chavrier, P., Parton, R. G., Hauri, H. P., Simons, K., and Zerial, M. (1990) *Cell* **62**, 317-329
 39. Méresse, S., Gorvel, J. P., and Chavrier, P. (1995) *J Cell Sci* **108**, 3349-3358
 40. Press, B., Feng, Y., Hoflack, B., and Wandinger-Ness, A. (1998) *J Cell Biol* **140**, 1075-1089
 41. Ceresa, B. P., Lotscher, M., and Schmid, S. L. (2001) *J Biol Chem* **276**, 9649-9654
 42. Grosshans, B. L., Ortiz, D., and Novick, P. (2006) *Proc Natl Acad Sci U S A* **103**, 11821-11827
 43. Eskelinen, E. L., Schmidt, C. K., Neu, S., Willenborg, M., Fuertes, G., Salvador, N., Tanaka, Y., Lullmann-Rauch, R., Hartmann, D., Heeren, J., von Figura, K., Knecht, E., and Saftig, P. (2004) *Mol Biol Cell* **15**, 3132-3145
 44. Levine, B. (2005) *Cell* **120**, 159-162
 45. Portnoy, D. A., Jacks, P. S., and Hinrichs, D. J. (1988) *J Exp Med* **167**, 1459-1471
 46. Pust, S., Morrison, H., Wehland, J., Sechi, A. S., and Herrlich, P. (2005) *Embo J* **24**, 1287-1300
 47. Tilney, L. G., and Portnoy, D. A. (1989) *J Cell Biol* **109**, 1597-1608
 48. Birmingham, C. L., Canadien, V., Kaniuk, N. A., Steinberg, B. E., Higgins, D. E., and Brumell, J. H. (2008) *Nature* **451**, 350-354
 49. Romano, P. S., Gutierrez, M. G., Beron, W., Rabinovitch, M., and Colombo, M. I. (2007) *Cell Microbiol* **9**, 891-909
 50. Prada-Delgado, A., Carrasco-Marin, E., Pena-Macarro, C., Del Cerro-Vadillo, E., Fresno-Escudero, M., Leyva-Cobian, F., and Alvarez-Dominguez, C. (2005) *Traffic* **6**, 252-265

51. Yamaguchi, H., Nakagawa, I., Yamamoto, A., Amano, A., Noda, T., and Yoshimori, T. (2009) *PLoS Pathog* **5**, e1000670
52. Limbago, B., Penumalli, V., Weinrick, B., and Scott, J. R. (2000) *Infect Immun* **68**, 6384-6390
53. Stassen, M., Muller, C., Richter, C., Neudorfl, C., Hultner, L., Bhakdi, S., Walev, I., and Schmitt, E. (2003) *Infect Immun* **71**, 6171-6177
54. Timmer, A. M., Timmer, J. C., Pence, M. A., Hsu, L. C., Ghochani, M., Frey, T. G., Karin, M., Salvesen, G. S., and Nizet, V. (2009) *J Biol Chem* **284**, 862-871
55. Ogawa, M., Yoshimori, T., Suzuki, T., Sagara, H., Mizushima, N., and Sasakawa, C. (2005) *Science* **307**, 727-731
56. Meyer-Morse, N., Robbins, J. R., Rae, C. S., Mocheгова, S. N., Swanson, M. S., Zhao, Z., Virgin, H. W., and Portnoy, D. (2010) *PLoS One* **5**, e8610
57. Neeman, R., Keller, N., Barzilai, A., Korenman, Z., and Sela, S. (1998) *Lancet* **352**, 1974-1977
58. Mizushima, N., Ohsumi, Y., and Yoshimori, T. (2002) *Cell Struct Funct* **27**, 421-429
59. Wang, C. W., and Klionsky, D. J. (2003) *Mol Med* **9**, 65-76

Footnotes

GAS strain JRS4 was kindly provided by Dr. E. Hanski (The Hebrew University, Jerusalem, Israel). The expression plasmids pOGW, pEGFP-LC3, and pmcherry-1 were given by Dr. S. Ishikawa (Nara Institute of Science and Technology, Nara, Japan), Dr. T. Yoshimori (National Institute for Basic Biology, Okazaki, Japan), and Dr. R. Y. Tsien, respectively. This work was partly supported by JSPS Grant-in-Aid for Scientific Research (B) (22390394), for Scientific Research (C) (22592032), for young scientists (B) (21792069), the Uehara Memorial Foundation, the Takeda Foundation and the Mitsubishi Foundation.

The following abbreviations are used: GAS, group A streptococcus; SLO, streptolysin O; LLO, listeriolysin O; EGFP, enhanced green fluorescent protein; DA, dominant active; DN, dominant negative; CFU, colony-forming unit; LC3, microtubule-associated protein 1 light chain 3; LAMP-1, lysosome associated membrane protein-1; EEA-1, early endosomal antigen-1; PI, propidium iodide; DAPI, 4', 6-diamino-2-phenylindole.

Figure legends

FIGURE 1. Localization of intracellular GAS and Rab proteins in HeLa cells. (A) HeLa cells expressing fluorescently labeled Rab5 (left panels) or Rab7 (right panels) were infected with GAS strain JRS4. The times shown in the figure indicate the elapsed time after infection. Rab proteins with EGFP are shown in green. Bacterial and host DNA was stained red with PI. Arrows indicate early endosomes (Rab5) or Rab7-positive compartments (Rab7) that contained bacteria. Arrowheads show bacteria in the cytoplasm. Inserts show magnified images of bacteria trapped by endosomes or free in the cytoplasm. Bars: 10 μm . The same images divided by color are shown in Supplemental fig. S1. (B) Cells expressing Rab5 were infected with JRS4 (open circles) or JRS4 Δ slo (closed circles) for the indicated period. The ratio of trapped GAS in endosomes to total intracellular bacteria was determined from confocal microscopic images. The *p*-value was determined by comparing cells infected with JRS4 Δ slo to those infected with JRS4 using Student's *t*-test (**p* < 0.05 and ***p* < 0.01).

FIGURE. 2. Localization of endosomal structures and LC3-positive compartments (indicating autophagosomes) in GAS-infected cells. (A, B) Cells expressing fluorescently labeled Rab5 (A), Rab7 (B), and LC3 (A, B) were infected with GAS strain JRS4. Early endosomes (A) and Rab7-positive endosomal structures (B) were labeled with EGFP (green). Autophagosomes were labeled with mCherry (red). Bacterial and host DNA was stained blue with DAPI. Arrowheads indicate bacteria surrounded by autophagosomes that were not within early endosomes (A) or that were also trapped in Rab7-positive compartments (B). Bars: 10 μm . The same images divided by color are shown in Supplemental figs. S2A and B. (C) JRS4-infected cells were observed by electron microscopy. Arrows and arrowheads indicate endosomes and autophagosomes, respectively. Capital 'F' shows bacteria in the cytoplasm. Bars: 1 μm .

FIGURE. 3. Influence of DA and DN mutants of Rab on the formation and maturation of early endosomes and bacterial invasion into GAS-infected cells. (A) Cells expressing Rab5Q79L (DA form of Rab5) (left panels) or Rab7Q67L (DA form of Rab7) (right panels) were infected with GAS strain JRS4. Endosomal structures were labeled with EGFP (green). Bacterial and host DNA was stained with PI (red). Lysosomes were indicated by LAMP1 stained with a specific antibody and cy5-conjugated secondary antibody (blue, data are shown in right panels). The same images divided by color are shown in Supplemental fig. S3. Bars: 10 μm . (B) Cells expressing Rab5, Rab5Q79L, Rab5S34N (DN form of Rab5), Rab7, Rab7Q67L, or Rab7T22N (DN form of Rab7) were infected with JRS4 for 1 h and incubated with antibiotics for an additional 10 min. The number of intracellular live JRS4 was counted, and the ratio of intracellular JRS4 to the number of bacteria added to the cell cultures is shown. Mock cells were transfected with empty vector prior to their infection with JRS4. *p*-values were determined by comparison with the cells expressing wild-type Rab proteins (**p* < 0.05) using Student's *t*-test.

FIGURE. 4. Localization of early endosomes, autophagosomes, and lysosomes in GAS-infected cells. (A, B) Cells expressing fluorescently labeled LC3 to indicate autophagosomes (A) or Rab5 to indicate early endosomes (B) were infected with JRS4 for 3 or 4 h. Autophagosomes or early endosomes were labeled with EGFP (green). Bacterial and host DNA were stained with PI (red). Cells were stained with anti-LAMP-1 to indicate lysosomes (A, B) (blue). The same images divided by color are shown in Supplemental figs. S5A and B. (A) Arrows and insets indicate autophagosomes sequestering bacteria and fused with lysosomes. (B) Arrows indicate LAMP-1 which containing intracellular bacteria but not co-localized within early endosomes. Arrowheads indicate early endosomes surrounding bacteria but not co-localized with LAMP-1. Insets show bacteria surrounded by LAMP-1, adjacent to early endosomes. Bars: 10 μ m.

FIGURE. 5. Influence of SLO on the induction of autophagy in GAS-infected cells. (A, B) Cells expressing LC3 were infected with one of the GAS strains, JRS4, JRS4 Δ slo (Δ slo), or JRS4 Δ slo-comp (comp). Bacterial and host DNA was stained with PI (red). Autophagosomes were visualized with EGFP (green). The same images divided by color are shown in Supplemental figs. S7A and B. Bars; 10 μ m. (A) Cells infected with JRS4 Δ slo were stained with an anti-LAMP-1 antibody to indicate lysosomes (blue). The insets show that bacteria were surrounded by lysosomes but not by autophagosomes. (B) Cells were infected with GAS for 2 h. EEA-1 was stained with a specific antibody to indicate early endosomes (blue). Arrows indicate early endosomes surrounding bacteria. Arrowheads indicate bacteria sequestered by autophagosomes. Insets show autophagosomes containing bacteria adjacent to endosomes (JRS4, comp) or bacteria only within endosomes (Δ slo). (C) Cells expressing fluorescently labeled LC3 to indicate autophagosomes were infected with JRS4 (open circles), JRS4 Δ slo (Δ slo; closed circles), or JRS4 Δ slo-comp (comp; open squares). Data are shown as the percentage of GAS-infected cells forming autophagosomes. p -values were determined by comparison with the percentage of cells infected with JRS4 Δ slo using the chi-square test ($*p < 0.05$, $**p < 0.01$, and $***p < 0.005$).

FIGURE. 6. Influence of SLO expression on bacterial viability in infected cells. (A-E) Cells were infected with JRS4 (open circles and bars) or JRS4 Δ slo (closed circles and bars) for 1 h and 10 minutes, 3 h (A, B, and D), or 5 h (A, C, and E). Data are shown as the percentage of GAS at 3 or 5 h after infection in comparison with that 10 min after the replacement of media (1 h and 10 min after infection). (B-E) Cells were transfected with plasmids expressing wild-type Rab5 (B, C), Rab5Q79L (B, C), wild-type Rab7 (D, E), or Rab7Q67L (D, E) prior to infection. Mock cells were transfected with empty vector. p -values were determined by comparison with the percentage of live JRS4 using Student's t -test ($*p < 0.05$, $**p < 0.01$, and $***p < 0.005$) or live JRS4 Δ slo in cells expressing wild-type Rab5 using Scheffe's test ($^{\#}p < 0.05$).

FIGURE. 7. The lack of SLO accumulation in endosomes influences the behavior of

intracellular GAS. (A, B) Cells expressing Rab5 (A) or Rab5Q79L (B) were infected with JRS4 (B) or JRS4 Δ slo (Δ slo) (A, B). Early endosomal structures were visualized with EGFP (green). Bacterial and cellular DNA was stained with PI (red). The same images divided by color are shown in Supplemental figs. S8A and B. Bars: 10 μ m. (A) Arrowheads and insets indicate bacteria located in early endosomes. (B) SLO was stained with a specific antibody (blue). Arrowheads and insets (JRS4) indicate the localization of SLO within endosomes. Arrow and inset in the image of JRS4 Δ slo-infected cells indicate endosomes without accumulated SLO.

FIGURE. 8. Schematic diagram of the endosomal and autophagic degradation pathway of intracellular GAS in HeLa cells. The illustration shows the intracellular behavior of GAS, including their invasion and escape into the cytoplasm (with SLO expression), in relation to the endosomal and autophagic degradation of GAS by the host cell. The involvement of both GDP- and GTP-bound form of Rab5 and Rab7 in each event is also indicated. The endosomal and autophagic pathways of GAS are depend on SLO expression and shown in thick lines. Blue arrows indicate the inhibition of these pathways by active or inactive Rab proteins.

Fig. 1 Sakurai et al.

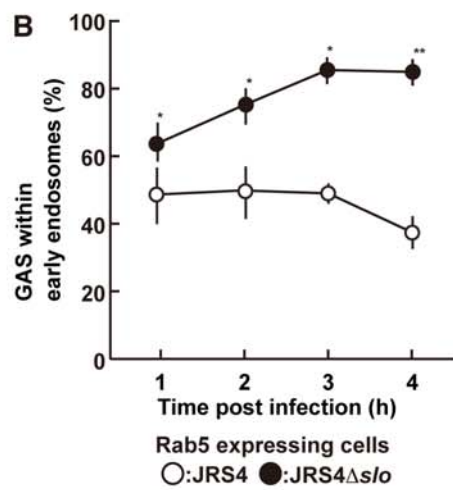
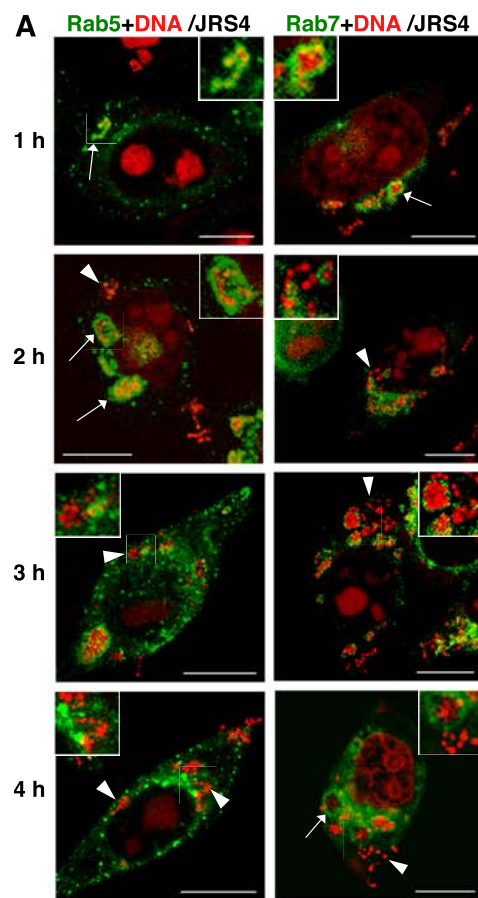


Fig. 2 Sakurai et al.

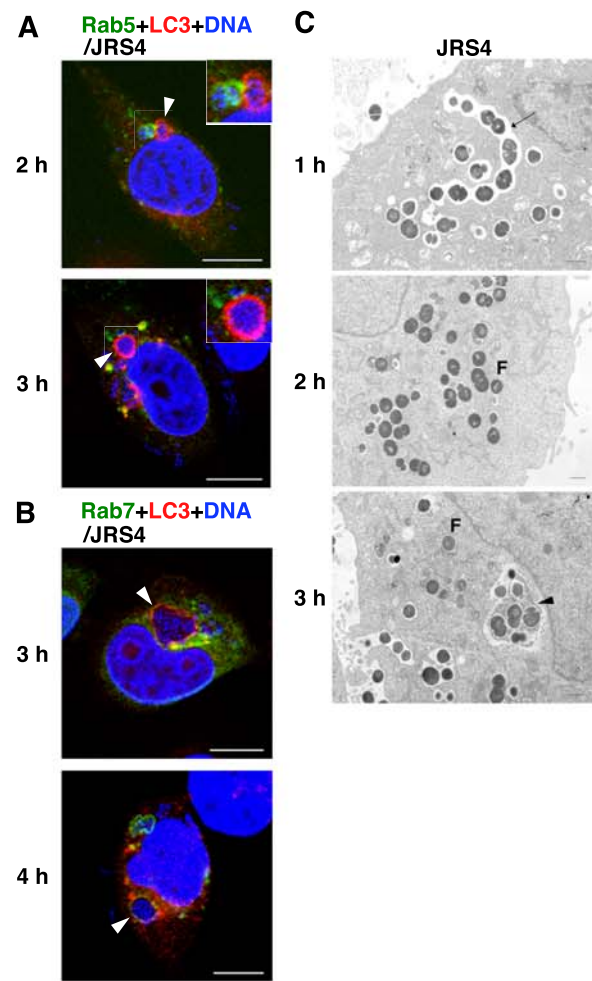


Fig. 3 Sakurai et al.

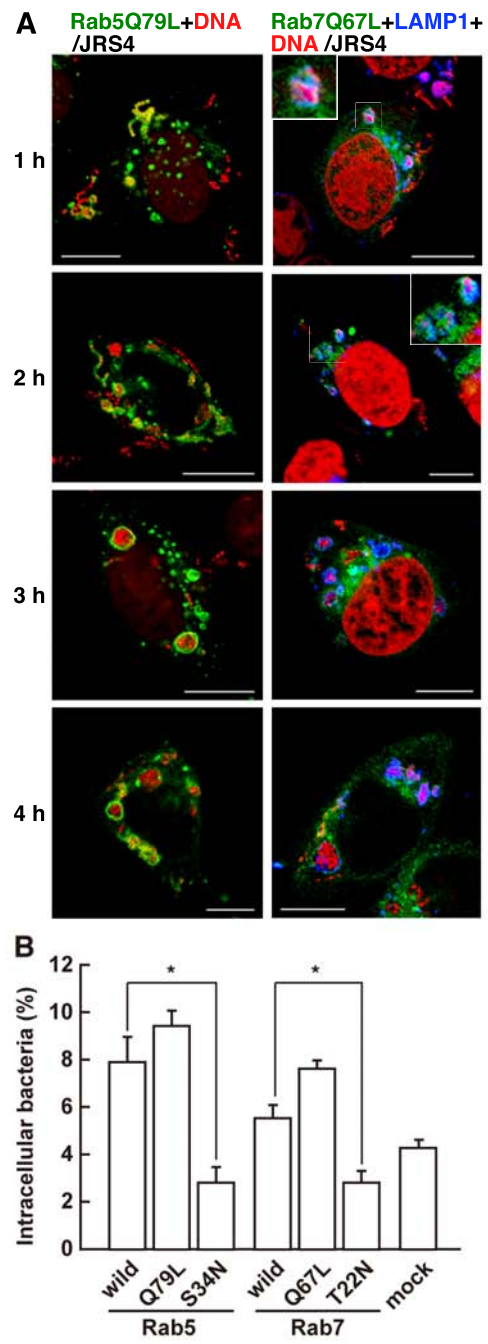


Fig. 4 Sakurai et al.

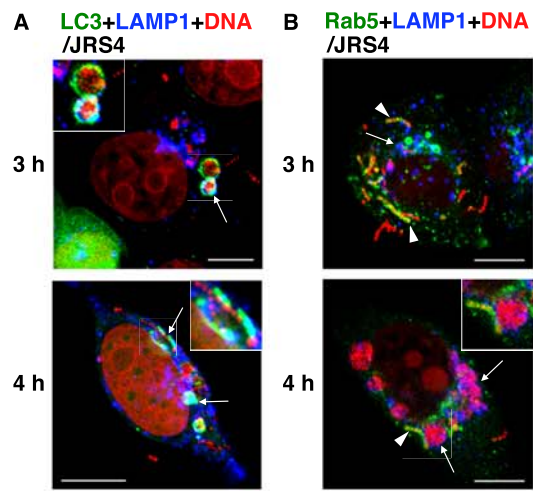


Fig. 5 Sakurai et al.

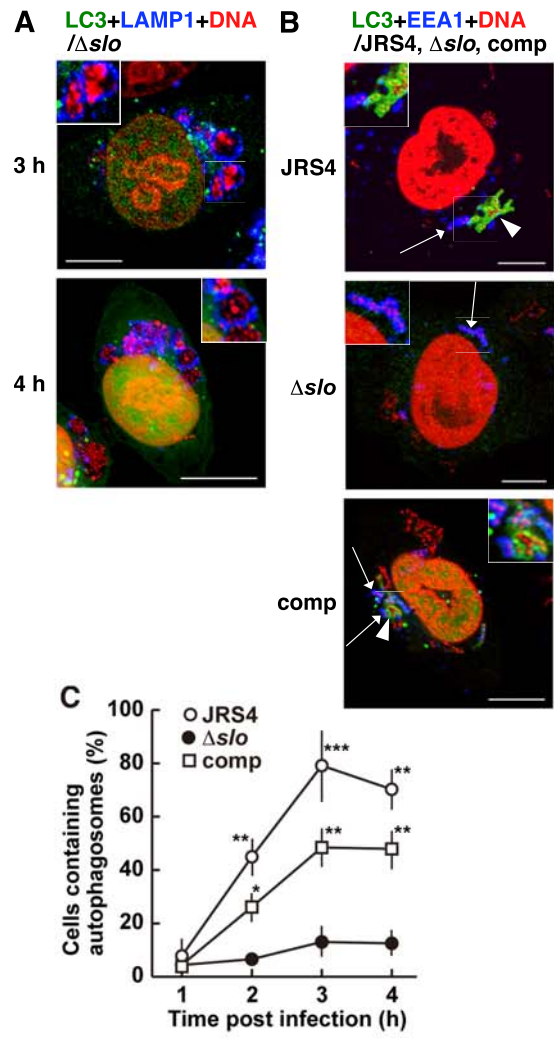


Fig. 6 Sakurai et al.

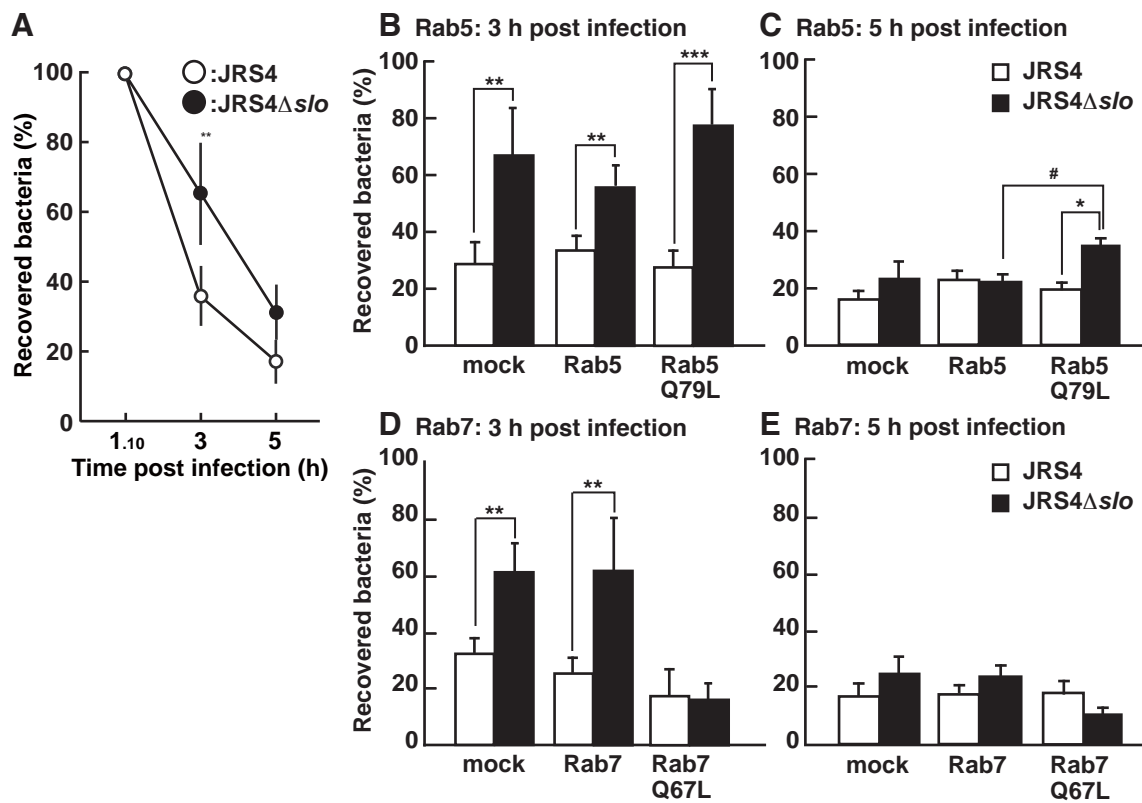


Fig. 7 Sakurai et al.

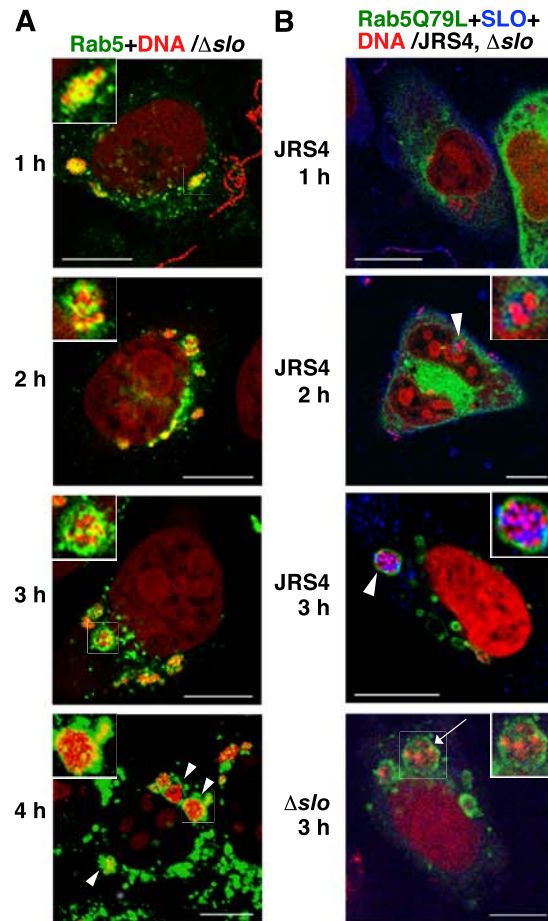
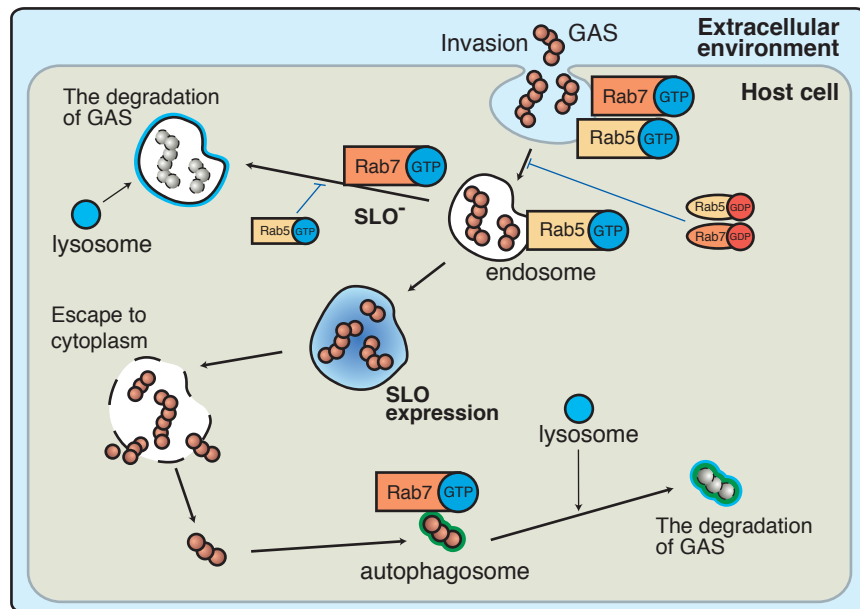


Fig. 8 Sakurai et al.



Supplemental figure legends

FIGURE. S1. Localization of intracellular GAS and Rab proteins in infected cells. HeLa cells expressing fluorescently labeled Rab5 (upper panels) or Rab7 (lower panels) were infected with JRS4 for the indicated period. Rab proteins are shown in green. Bacterial and host DNA were stained red. The merged images are also shown in Fig. 1A. Bars: 10 μm .

FIGURE. S2. Localization of endosomal structures and autophagosomes in GAS-infected cells. (A, B) Cells expressing fluorescently labeled Rab5 (A), Rab7 (B), and LC3 (A, B) were infected with JRS4 for the indicated period. Rab proteins and autophagosomes are shown in green and red, respectively. Bacterial and host DNA were stained blue. Merged images are also shown in Figs. 2A and B. Bars: 10 μm .

FIGURE. S3. Influence of DA mutants for Rab expression on the formation and maturation of early endosomes in GAS-infected cells. Cells expressing fluorescently labeled Rab5Q79L (upper panels) or Rab7Q67L (lower panels) were infected with JRS4. Rab proteins are shown in green. Bacterial and host DNA were stained red. Cells expressing Rab7Q67L were also stained with an anti-LAMP-1 antibody to indicate lysosomes (blue). Merged images are also shown in Fig. 3A. Bars: 10 μm .

FIGURE. S4. Influence of DN mutants for Rab expression on the bacterial invasion into cells and fusion of Rab7-positive compartments with lysosomes. (A, B) Cells expressing Rab5S34N (A) or Rab7T22N (B) were infected with JRS4 for the indicated periods. Rab5S34N (A) or Rab7T22N (B) was visualized with EGFP (green). Bacterial and cellular DNA was stained with PI (red). In (B), cells were also stained with an anti-LAMP-1 antibody to indicate lysosomes (blue). Bars: 10 μm .

FIGURE. S5. Localization of early endosomes, autophagosomes, lysosomes, and a lysosomal enzyme in GAS-infected cells. (A-C) Cells expressing fluorescently labeled LC3, a marker of autophagosomes (A, C) or Rab5, a marker of early endosomes (B) were infected with JRS4 for 3 or 4 h. Autophagosomes or early endosomes are shown in green. Bacterial and host DNA were stained red. To label lysosomes, an anti-LAMP-1 (A, B) and an anti-cathepsin D antibody (C) were used (blue). (A, B) Merged images are also shown in Figs. 4A and B. Bars: 10 μm . (C) Arrows and insets show bacteria sequestered by autophagosomes, where cathepsin D was

also localized. Bars: 10 μ m.

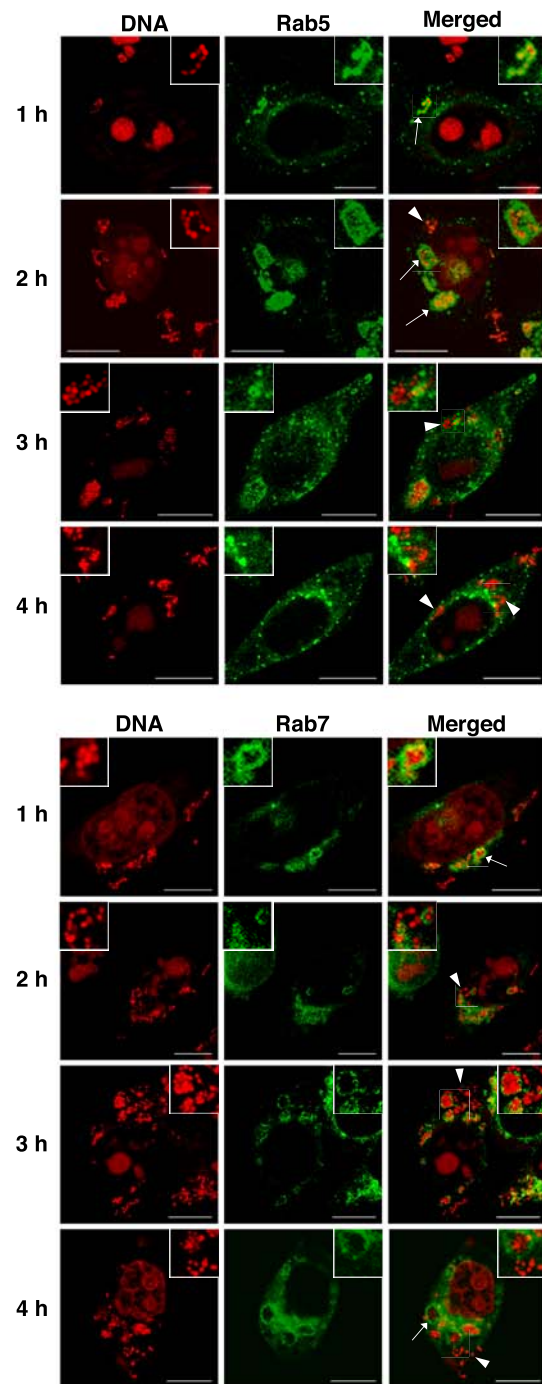
FIGURE. S6.

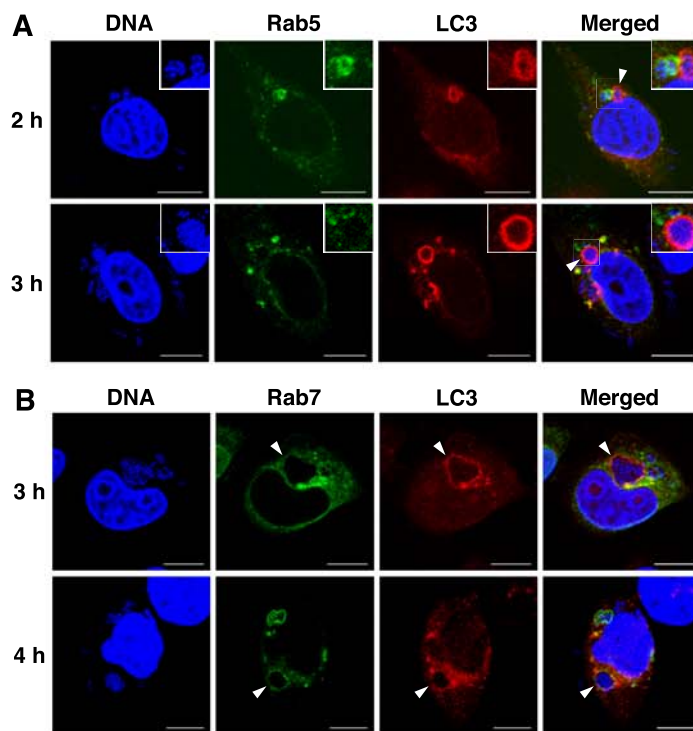
Confirmation of *slo*-complemented strain of JRS4 Δ *slo*. (A) SDS-PAGE and Western blot analyses of *E. coli* strains. DH10B was transformed with pOGW-SLO, and the transformants were incubated with (+) or without (-) 1 mM IPTG. Coomassie brilliant blue (CBB) staining and western blot using an anti-SLO peptide antibody are shown. 'M' indicates a molecular marker at 62 kDa. (B) PCR and western blot analysis of JRS4, JRS4 Δ *slo* (Δ *slo*), and JRS4 Δ *slo*-comp (comp). The *slo* gene in each GAS strain was assessed by PCR, and the expression of SLO protein in culture supernatants with (+) or without (-) 1 mM IPTG was examined by western blotting using a specific antibody.

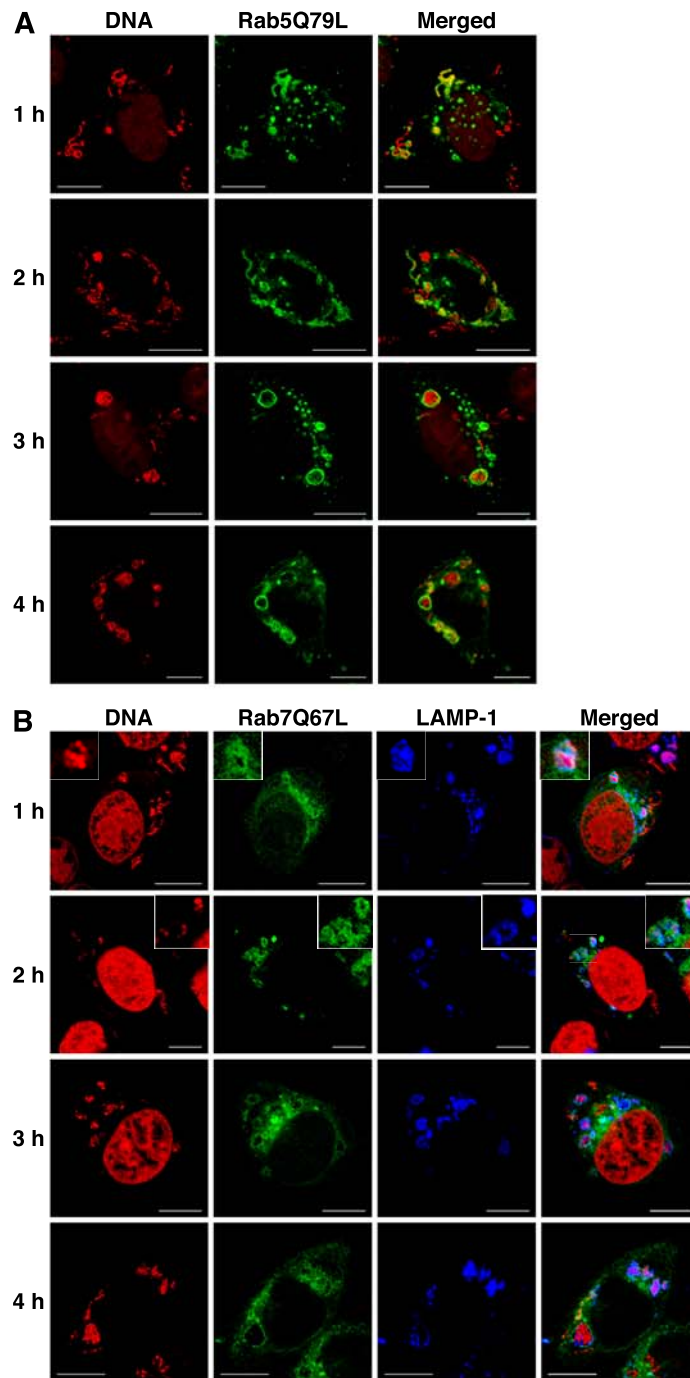
FIGURE. S7. Influence of SLO on the induction of autophagy in GAS-infected cells. (A, B) Cells expressing fluorescently labeled LC3 to indicate autophagosomes were infected with each GAS strain, JRS4, JRS4 Δ *slo* (Δ *slo*), or JRS4 Δ *slo*-comp (comp) for 2 (B), 3, or 4 h (A). Autophagosomes are shown in green. Bacterial and host DNA were stained red. Anti-LAMP-1, to indicate lysosomes (A) and anti-EEA-1, to indicate early endosomes (B) antibodies were used (blue). Merged images are also shown in Figs. 5A and B. Bars: 10 μ m.

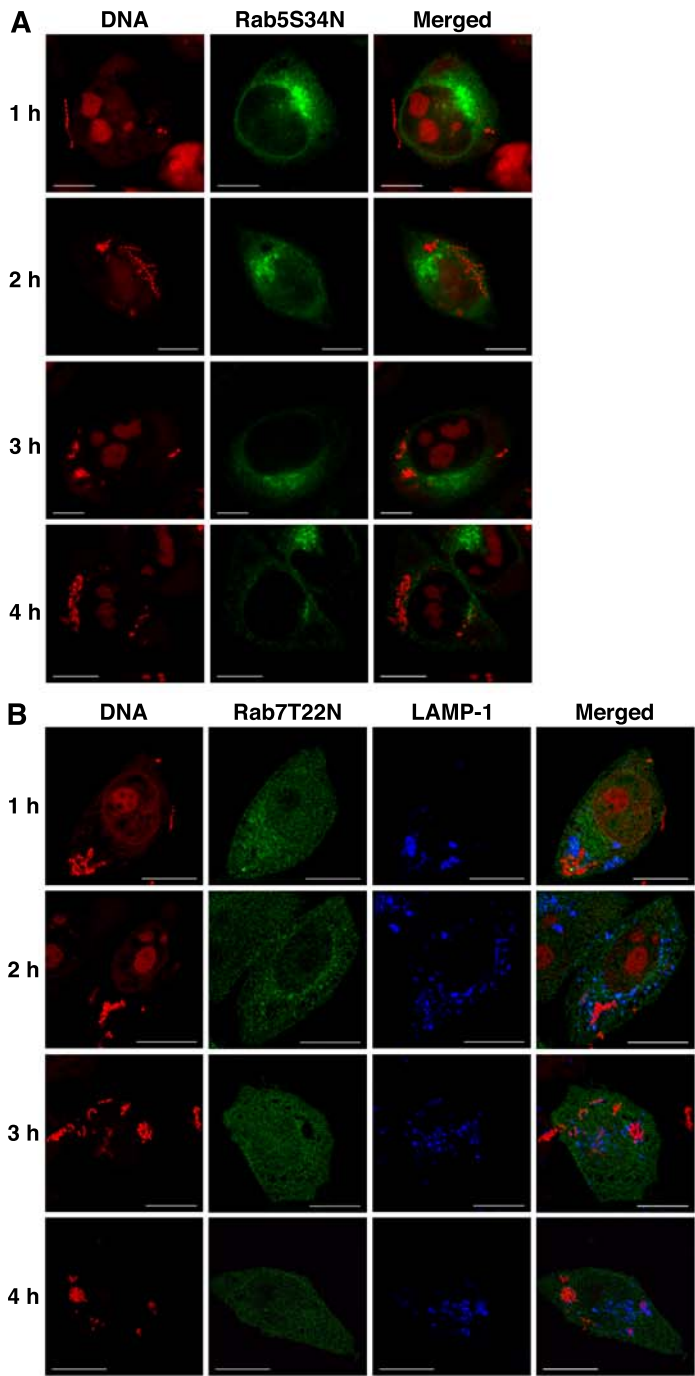
FIGURE. S8. The lack of SLO accumulation in endosomes influences the behavior of intracellular GAS. (A, B) Cells expressing Rab5 (A) or Rab5Q79L (B) were infected with JRS4 (B) or JRS4 Δ *slo* (Δ *slo*) (A, B). Rab proteins are shown in green. Bacterial and host DNA were stained red. In (B), an anti-SLO antibody was used to indicate lysosomes (blue). Merged images are also shown in Figs. 7A and B. Bars: 10 μ m.

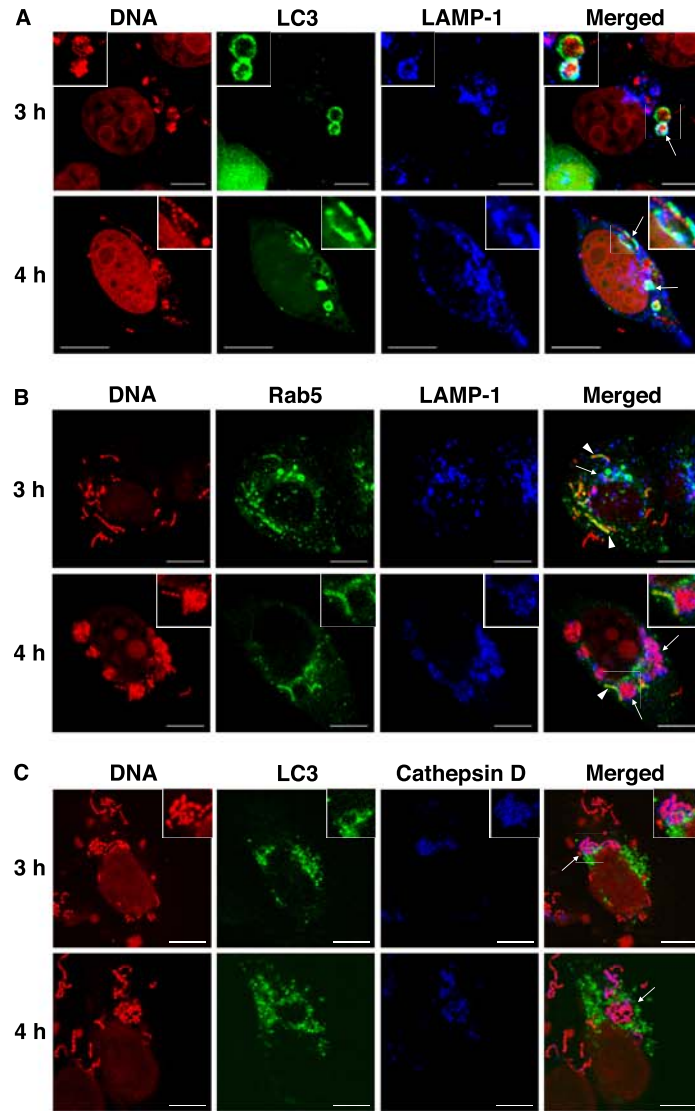
FIGURE. S9. Persistence of the *slo*-deficient mutant JRS4 strain in endosomal structures of cells. (A, B) Cells expressing Rab5Q79L (A) or wild-type Rab7 (B) were infected with JRS4 Δ *slo*. Endosomal structures were visualized with EGFP (green). Bacterial and host DNA were stained with PI (red). Insets show bacteria located in early endosomal structures (A) or Rab7-positive compartments (B). Bars: 10 μ m. (C) JRS4 Δ *slo*-infected cells were observed by electron microscopy. Arrows indicate endosomes surrounding bacteria. Bars: 1 μ m.

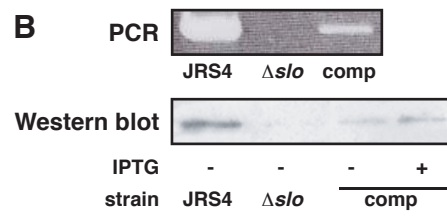
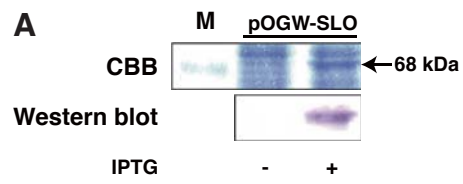


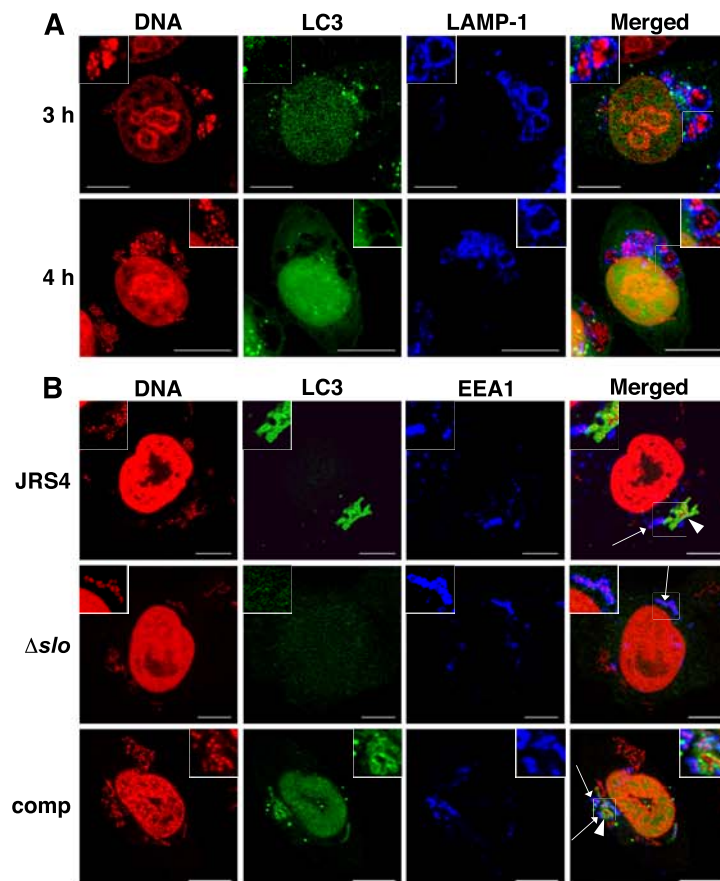


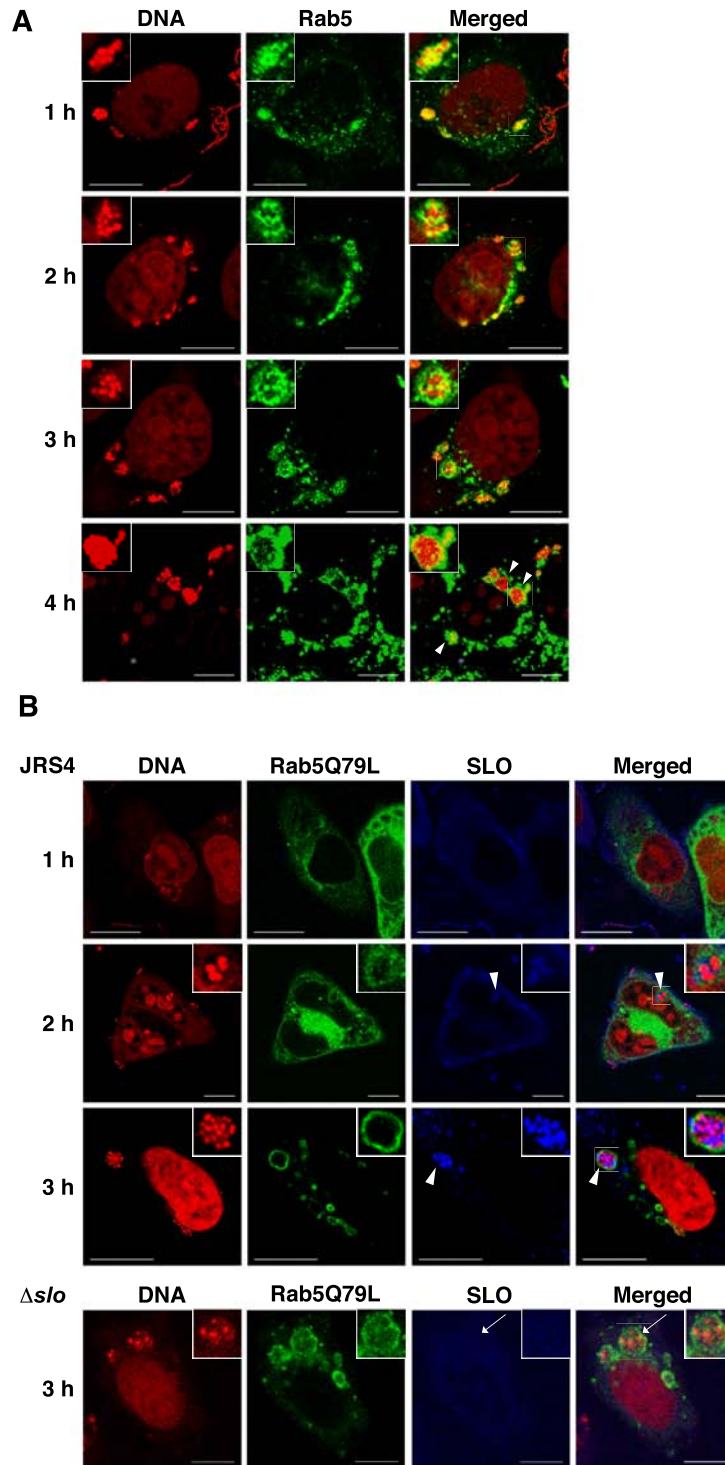


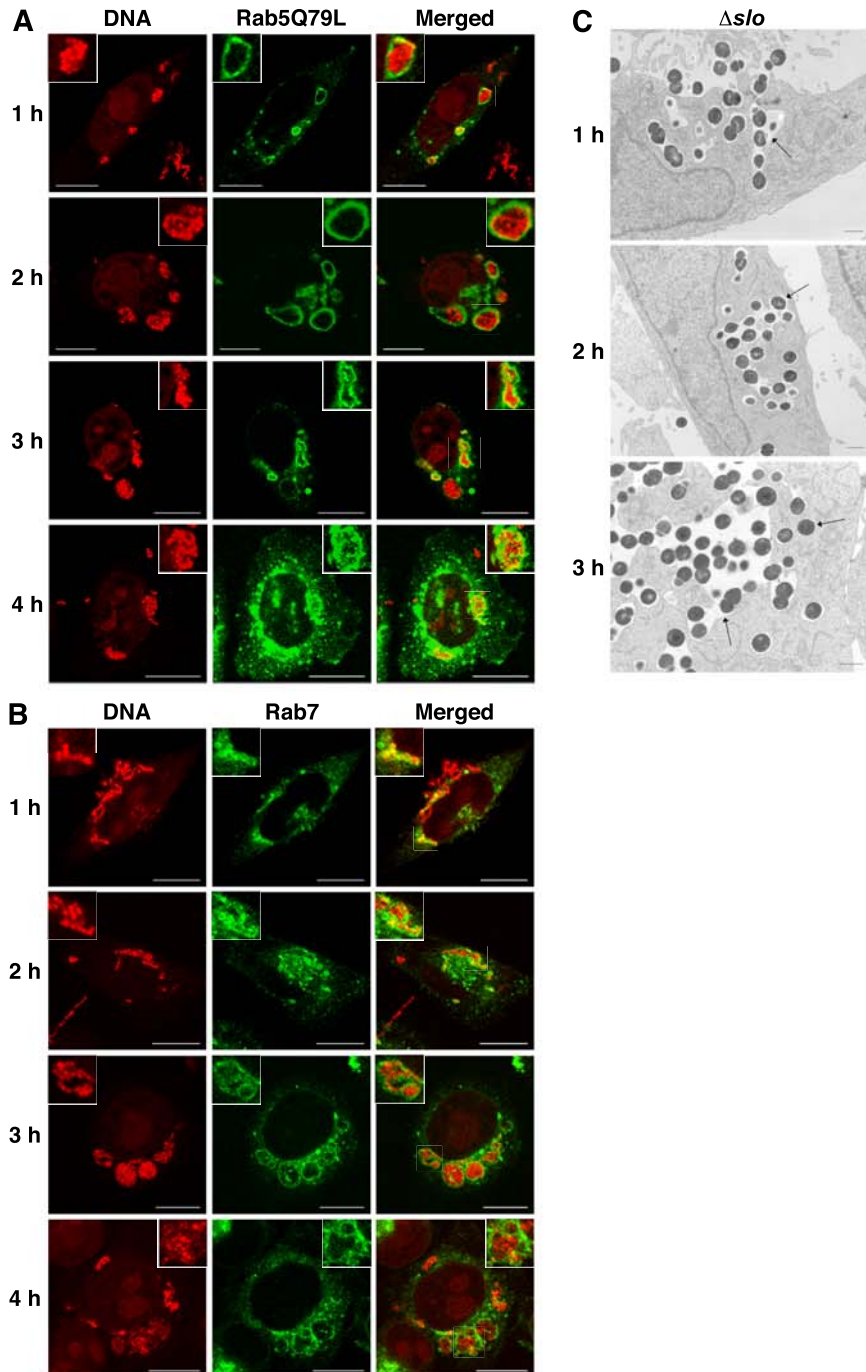












1 Supplemental table S1. Bacterial strains and plasmids used in this study.

2		Description	Antibiotics*	Reference
3	GAS strains			
4	JRS4	M6 strain.	Sm	26
5	JRS4 Δ <i>slo</i>	SLO-defective mutant of JRS4.	Sm, Km	This study
6	JRS4 Δ <i>slo</i> -comp	JRS4 Δ <i>slo</i> with an IPTG-inducible SLO-expressing-plasmid.	Sm, Km, Tet	This study
7				
8	<i>E. coli</i>			
9	DH10B	Plasmid construction and propagation.	-	Invitrogen
10				
11	Plasmids			
12	pSF151	Shuttle vector for the construction of GAS mutant strains.	Km	27
13	pSF151-fSLO	pSF151 harboring an internal fragment of <i>slo</i> gene.	Km	This study
14	pENTR-SD-TOPO	Cloning vector adapted for Gateway system.	Km	Life Tech
15	pOGW	IPTG inducible vector for protein expression.	Tet	29
16	pOGW-SLO	pOGW harboring intact <i>slo</i> gene.	Tet	This study
17	pEGFP-LC3	Expression plasmid for EGFP-fused LC3.	Km	30
18	pmCherry-1	Vector for the expression of mCherry-fused protein.	Km	Clontech
19	pmCherry-LC3	Expression plasmid for mCherry-fused LC3.	Km	This study
20	pENTR11	Cloning vector adapted for Gateway system.	Km	Life Tech
21	pENTR-EGFP-LC3	pENTR11 harboring EGFP-fused LC3 expressing gene.	Km	This study
22	pKF19K	Vector used for the induction of mutation.	Km	Takara
23	pcDNA3.1 Zeo(+)	Vector for protein expression.	Amp	Life Tech
24	pcDNA3.1 Zeo(+)- EGFP-Rab5	Expression plasmids for EGFP-fused Rab5.	Amp	This study
25				
26	pcDNA3.1 Zeo(+)- EGFP-Rab5Q79H, Rab5S34N	Expression plasmids for EGFP-fused mutant Rab5.	Amp	This study
27				
28	pcDNA3.1 Zeo(+)- EGFP-Rab7	Expression plasmids for EGFP-fused Rab7.	Amp	This study
29				
30	pcDNA3.1 Zeo(+)- EGFP-Rab7Q67L, Rab7T22N	Expression plasmids for EGFP-fused mutant Rab7.	Amp	This study
31				
32	pAd/CMV/V5-DEST	Plasmid for protein-expressing adenovirus.	Amp	Life Tech

1 Supplemental table S1, continued.

2		Description	Antibiotics*	Reference
3	pAd-EGFP-	Plasmid for the production of Rab5 protein-expressing-	Amp	This study
4	Rab5	adenovirus.		
5	pAd-EGFP-	Plasmids for the production of mutant Rab5 protein-expressing-	Amp	This study
6	Rab5Q79H, Rab5S34N	adenovirus.		
7	pAd-EGFP-	Plasmid for the production of Rab7 protein-expressing-	Amp	This study
8	Rab7	adenovirus.		
9	pAd-EGFP-	Plasmids for the production of mutant Rab7 protein-expressing-	Amp	This study
10	Rab7Q67L, Rab7T22N	adenovirus.		

11 *Antibiotics; Resistance to antibiotics.

12 Abbreviations: Sm, Streptomycin; Amp, ampicillin; Km, Kanamycin; Tet, Tetracycline; Life Tech, Life Technologies.

1 Supplemental table S2. Sequences of synthetic oligonucleotides used for PCR and mutagenesis.

2	Target gene or purpose	Primer sequence
3	<i>slo</i> , internal fragment	5'- <u>GAGAA</u> TTTCGAGCGAAGAAGATCACACTGAAGA
4		5'- <u>GAGGAT</u> CCGCTTGTATGCTGCAATCATCACCT
5	Rab5	5'-CACCATGGCTAGTCGAGGCGCAACAAGA
6		5'-TTAGTTACTACAACACTGATTCCTGGTT
7	Rab7	5'-CACCATGACCTCTAGGAAGAAAGTGTTG
8		5'-TCAGCAACTGCAGCTTCTGCCGAGGCC
9	Intact <i>slo</i>	5'-CACCCACCATGAAGGACATGTCTAATAAAAAAACATTT
10		5'-CTACTTATAAGTAATCGAACCATATGGGCT
11	Rab5Q67L	5'- GCTGGT <u>CT</u> AGAACGATACCATAGCCTA
12		5'- TCGTT <u>CT</u> AGACCAGCTGTATCCCATAT '
13	Rab5S34N	5'- GGCAAAA <u>AT</u> AGCCTAGTGCTTCGTTTT
14		5'- TAGGCT <u>AT</u> TTTTGCCAACAGCGGACTC
15	Rab7Q67L	5'- GCAGG <u>ACT</u> CGAACGGTTCAGTCTCTC
16		5'- CCGTTC <u>GAG</u> TCCTGCTGTGTCCCATAT
17	Rab7T22N	5'- GGGAAG <u>AAT</u> CACTCATGAACCAGTAT
18		5'- AGTGA <u>ATT</u> CTTCCCGACTCCAGAATC

19
20 Underlines show restriction enzyme sites or mutagenesis sites.